NEW APPROACH FOR 3D OBJECT RECOGNITION USING NON UNIFORM FOURIER AND MOMENTS COEFFICIENTS

KHALID AZNAG*, NOUHOUN KANE, AHMED EL OIRRAK,
ESSAID EL BACHARI

Faculty of Sciences Semlalia, Cadi Ayyad University, Computer Systems Engineering
Laboratory (LISI) Marrakech, Morocco
*Corresponding Author: Khalid.aznag@ced.uca.ac.ma

Abstract

In this paper, new descriptors have been proposed which are invariant to rotation and affinity transformations (Non Uniform Fourier and moments coefficients). These descriptors are computed using Fourier or moments coefficients obtained from development of object coordinates. These coordinates are parameterized with a function also invariant to affinity. The normal Fourier transform depends on points index, the Non Uniform transform proposed here depend on a parameter. This parameter depends on shape not on order of points. The proposed descriptors are easy to extract and are extensible to higher dimension.

Keywords: Fourier, Rotation-invariant, 3D curve, Non Uniform transform.

1. Introduction

The development of computer animations and computer graphics has made 3D models as images and video. Therefore, it is needful to design an automatic 3D model retrieval system which enables the users to search interested 3D models effectively. Research in the 3D objects databases has attracted several works [1-3]. Search by content is one of the latest methods [4-6]. It allows searching of 3D object visually similar to a query object. The important step in content search is to find adequate descriptor which can discriminate between objects. It is to find a 3D shape descriptor to measure the similarity between the elements of 3D object-based. Shih et al. [7] proposed a 3D model retrieval system based on the 3D angular radial transform (3D-ART) and 3D discrete Fourier transform (3D-DFT). Several methods of ordinary Fourier transforms are used for searching and indexing 3D objects [8-10]. In this work, we use Non Uniform Fourier Transform

Nomenclatures

T	The period (the time needed for one cycle. Units: radians)
X	A set of 3D points
$\tilde{X}$	The transformed set
x, y, z	Cartesian coordinates

Greek Symbols

δ_k	Kronecker-Symbol
θ	Angle
τ	Parameter used into development

Abbreviations

DFT	Discrete Fourier Transform
FD	Fourier Descriptors
FS	Fourier Series
NUFT	Non Uniform Fourier Transform
U	Fourier Transform for x
V	Fourier Transform for y
W	Fourier Transform for z

(NUFT), the usefulness of NUFT will be highlighted with a 3D or Set of points. EL oirrak use the affine-invariant FD to take into consideration affine shape distortion [11, 12] but only for structured data. In this work, we extend the recognition processes to handle unstructured data. The need for recognition from irregularly spaced data [13, 14] occurs in many different fields, such as cartography, medical imaging, meteorological or geological modelling and computer aided geometric design. For example, in meteorology weather measurements are available from irregularly located observation stations. In geostatistics and geology, aquifer properties and layer structures are studies from data that is only available at a few given locations. The data at these few locations are used in order to allow the use of 3D or 2D scientific visualization tools to illustrate the variation in the data. The scattered data are typical of observational data that are scattered at irregular locations in two or three dimensions (i.e., data with no notion of connectivity or topology). From a set of points, we can have different shapes.

In addition, these sets of points are recognized without taking into consideration the shape. To do this, we try to adapt the methods of Fourier descriptors to handle irregular sampling (unstructured data) and 3D space. Thus, we define Fourier Descriptors (FD) and Fourier Series (FS) for point set. From a computational point of view, the difference between regular FD and irregular FD is; unlike the presence of an integer index in the regular case, the irregular case contains a parameter which depend on shapes appears in the exponent. We also generalize the method of moments by allowing derivation of high order moments. Geometric moment invariants have attracted wide attention and have been used in many applications, pose estimation, character recognition, quality inspection in industrial areas, matching, etc. Historically, Hu published the first significant paper on the use of image moment invariants for two-dimensional pattern recognition applications [15]. The main advantage of our approach is that it is

systematic and it allows obtaining the analytical form of all invariant polynomials of a given order, which was not the case using Flusser and Suck method [16]. The proposed moments are also easy to compute compared to Hu moments or Fulsser moments [17, 18]. Hu moments are invariant under rotation, and are limited to first order moment. Flusser moments are invariant under affinity and are also limited to first order moments. In general we have two cases:

a) Structured set of points, indexed by *n* integer which represent the order of a points,

b) Unstructured set of points, in this case the order is not respected and we propose the use of another characteristic of a point, which is independent of the order.

The rest of the paper is organized as follows: In section 2, we describe some definitions of Fourier Descriptors. Novel Fourier Transform is presented in Section 3. Section 4 describes definitions of Novel Moments. Section 5 describes definitions of Novel Fourier Series. In section 6, we apply the proposed approach. Section 7 contains the conclusion and the future works.

2. Normal Fourier Descriptors (FD)

Definition:

To define FD for 3D parameterized point set; Let $X(n) = (x(n), y(n), z(n))$ $n=1...N$, be a closed 3D set of point with N a size (number of points on the normalized contour) and 2π as length. Then the Fourier descriptors are given by Eqs. (1), (2), (3) and (4):

$$Z(k) = \begin{pmatrix} u(k) \\ v(k) \\ w(k) \end{pmatrix} \tag{1}$$

with:

$$u(k) = \frac{1}{N} \sum_{n=1}^{N} x(n) e^{-j\frac{2\pi kn}{N}} \tag{2}$$

$$v(k) = \frac{1}{N} \sum_{n=1}^{N} y(n) e^{-j\frac{2\pi kn}{N}} \tag{3}$$

$$w(k) = \frac{1}{N} \sum_{n=1}^{N} z(n) e^{-j\frac{2\pi kn}{N}} \tag{4}$$

where *u*, *v* and *w* represent the FDs of *x*, *y* and *z* respectively and ($k = 0,..., N$).

Shift theorem:

If X and $\tilde{X}$ are two objects having the same shape, with a shift in starting point then (Eqs. (5), (6) and (7)):

$$\tilde{Z}(k) = e^{jkl_0} A Z(k) + B\delta_k \tag{5}$$

for all integer k,

$$Z(k) = \big(u(k), v(k), w(k)\big) \tag{6}$$

and

$$\tilde{Z}(k) = \big(\tilde{u}(k), \tilde{v}(k), \tilde{w}(k)\big) \tag{7}$$

Are respectively the bi dimensional FDs vectors of X and $\tilde{X}$.

3. Novel Fourier Transform

As normal Fourier transform is dependent on point index, so to solve this problem we apply a non uniform Fourier transform. Here we define this new Fourier transform and in section 6 we present implementation.

Definition:

In order to define FD for 3D parameterized point set; if $X(\tau) = \big(x(\tau), y(\tau), z(\tau)\big)$ denote a 3D set of point having τ as parameter and N as size (ie: number of points), then the Fourier descriptors are given by Eq. (8):

$$\begin{cases} u(k) = \frac{1}{N}\sum_{\tau} x(\tau)e^{-j\frac{k\tau}{T}} \\ v(k) = \frac{1}{N}\sum_{\tau} y(\tau)e^{-j\frac{k\tau}{T}} \\ w(k) = \frac{1}{N}\sum_{\tau} z(\tau)e^{-j\frac{k\tau}{T}} \end{cases} \tag{8}$$

where $T = \int \tau d\tau$

4. Novel Moments

Here we define a novel moments; the moments in our case cannot be defined for indexed set of point or are not exploitable so we present in the following the definition of geometric moments for 3D parameterized set of points, where the index of points can change.

Definition:

In order to define moment for 3D parameterized point set; if $X(\tau) = \big(x(\tau), y(\tau), z(\tau)\big)$ denote a 3D set of point having τ as parameter the moments in the directions *x*, *y* and *z* are given by Eqs. (9) and (10):

$$m_p^x = \int_{\tau} \tau^p x(\tau)d\tau \ , \ m_p^y = \int_{\tau} \tau^p y(\tau)d\tau \text{ and } m_p^z = \int_{\tau} \tau^p z(\tau)d\tau \tag{9}$$

Where *p* is the order of moments.

$$m_0^x = \int_{\tau} x(\tau)d\tau \ , \ m_0^y = \int_{\tau} y(\tau)d\tau \text{ and } m_0^z = \int_{\tau} z(\tau)d\tau \tag{10}$$

Linearity:

Let $X(\tau) = \big(x(\tau), y(\tau), z(\tau)\big)$ and $\tilde{X}(\tau) = \big(\tilde{x}(\tau), \tilde{y}(\tau), \tilde{z}(\tau)\big)$ with $(\tilde{x}, \tilde{y}, \tilde{z})$ as transformed coordinates denoting of 3D set of point, having τ as parameter and with an affine transform difference i.e:

$$\tilde{X} = AX \tag{11}$$

where

$$A = \begin{pmatrix} a_{11} & a_{12} & a_{13} \\ a_{21} & a_{22} & a_{23} \\ a_{31} & a_{32} & a_{33} \end{pmatrix} \tag{12}$$

denotes 3D affinity matrix .

Thus

$$\tilde{x} = a_{11}x + a_{12}y + a_{13}z \tag{13}$$

$$\tilde{y} = a_{21}x + a_{22}y + a_{23}z \tag{14}$$

$$\tilde{z} = a_{31}x + a_{32}y + a_{33}z \tag{15}$$

So

$$\begin{aligned}
m_p^{\tilde{x}} &= \int_\tau \tau^p \tilde{x}(\tau)d\tau \\
&= a_{11}\int_\tau \tau^p x(\tau)d\tau + a_{12}\int_\tau \tau^p y(\tau)d\tau + a_{13}\int_\tau \tau^p z(\tau)d\tau \\
&= a_{11}m_p^x + a_{12}m_p^y + a_{13}m_p^z
\end{aligned} \tag{16}$$

The same for $m_p^{\tilde{y}}$ and $m_p^{\tilde{z}}$. The parameter τ is chosen to be invariant under affinity. The affine arc length developed by Mokhtarian and Abbasi [19] is suitable for affinity case.

5. Fourier Series

In this section, we define FS for 3D point set, so the Fourier series are given by Eqs. (17), (18), (19), (20), (21) and (22):

$$FS\big(x(\tau)\big) = a_0^x + \sum_{n=1}^\infty \left(c_n^x e^{j\frac{n\tau}{T}} + c_{-n}^x e^{-j\frac{n\tau}{T}} \right) \tag{17}$$

$$FS\big(y(\tau)\big) = a_0^y + \sum_{n=1}^\infty \left(c_n^y e^{j\frac{n\tau}{T}} + c_{-n}^y e^{-j\frac{n\tau}{T}} \right) \tag{18}$$

$$FS\big(z(\tau)\big) = a_0^z + \sum_{n=1}^\infty \left(c_n^z e^{j\frac{n\tau}{T}} + c_{-n}^z e^{-j\frac{n\tau}{T}} \right) \tag{19}$$

where

$$\begin{cases} a_n^x = \int_\tau x(\tau)\cos(\dfrac{n\tau}{T})d\tau \\[3mm] b_n^x = \int_\tau x(\tau)\sin(\dfrac{n\tau}{T})d\tau \end{cases} \tag{20}$$

$$\begin{cases} a_n^y = \int_\tau y(\tau)\cos(\dfrac{n\tau}{T})d\tau \\[4mm] b_n^y = \int_\tau y(\tau)\sin(\dfrac{n\tau}{T})d\tau \end{cases} \tag{21}$$

$$\begin{cases} a_n^z = \int_\tau z(\tau)\cos(\dfrac{n\tau}{T})d\tau \\[4mm] b_n^z = \int_\tau z(\tau)\sin(\dfrac{n\tau}{T})d\tau \end{cases} \tag{22}$$

6. Results and Discussion

6.1. Application on set of points

In this work, we have four sets of 3d points (in *x, y, z*) coordinates shown in Fig. 1. We present our experiment test of our approach in two shapes Figs. 1(a) and (b). Using Eq. (23), the parameter used in this experiment is:

$$\tau = \sqrt{x^2 + y^2 + z^2} \tag{23}$$

In Tables 1 and 2, we present the *x*, *y* and *z* coordinates of the points with different indices of the two shapes, Figs. 1(a) and (b). In Table 3, we present the polar radius for each point. In Tables 4 and 5, we present the values of normal Fourier Transform for each shape, we can show no equality of coefficients. In Tables 6 and 7, we present the values of the novel Fourier Transform for each shape. We see that novel three components *U*, *V* and *W* are the same for two shapes Figs. 1(a) and (b). From Tables 4 to 7, it can be seen that the proposed Fourier Transform solve index point problem, so Non Uniform Fourier Transform is better than Normal Fourier Transform.
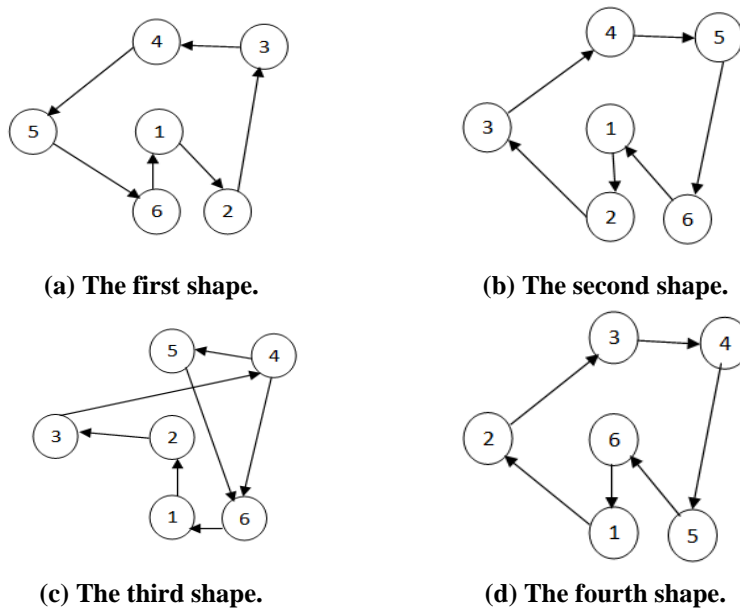

(a) The first shape.　　　　　　(b) The second shape.

(c) The third shape.　　　　　　(d) The fourth shape.

Fig. 1. A set of 6 points with associated shapes.

Table 1. Coordinates *x*, *y* and *z* for shape, Fig. 1(a).

Index	1	2	3	4	5	6
Coordinates *x*	1	1	0	1	2	1.5
Coordinates *y*	1	0	1	2	2	0
Coordinates *z*	0	1	1	0	0	1

Table 2. Coordinates *x*, *y* and *z* for shape, Fig. 1(b).

Index	1	2	3	4	5	6
Coordinates *x*	1	1.5	2	1	0	1
Coordinates *y*	1	0	2	2	1	0
Coordinates *z*	0	1	0	0	1	1

Table 3. Radius of shape, Fig. 1(a) and shape, Fig. 1(b).

for shape 1(a)	1.4142	1.4142	1.4142	2.2361	2.8284	1.8028
for shape 1(b)	1.4142	1.8028	2.8284	2.2361	1.4142	1.4142

Table 4. Normal Fourier transform of shape, Fig. 1(a).

U	V	W
0.3333 + 0.1443i	-0.0833 + 0.4330i	-0.0833 - 0.1443i
-0.1667 + 0.1443i	-0.2500 - 0.1443i	0.2500 + 0.1443i
0.0833 - 0.0000i	-0.3333 - 0.0000i	0.1667 + 0.0000i
-0.1667 - 0.1443i	-0.2500 + 0.1443i	0.2500 - 0.1443i
0.3333 - 0.1443i	-0.0833 - 0.4330i	-0.0833 + 0.1443i
1.0833 + 0.0000i	1.0000 + 0.0000i	0.5000 + 0.0000i

Table 5. Normal Fourier transform of shape, Fig. 1(b).

U	V	W
-0.2917 - 0.2165i	-0.3333 + 0.2887i	0.1667 + 0.0000i
0.2083 - 0.0722i	0.0000 - 0.2887i	-0.0000 + 0.2887i
0.0833 + 0.0000i	-0.3333 - 0.0000i	0.1667 - 0.0000i
0.2083 + 0.0722i	-0.0000 + 0.2887i	0.0000 - 0.2887i
-0.2917 + 0.2165i	-0.3333 - 0.2887i	0.1667 + 0.0000i
1.0833 + 0.0000i	1.0000 + 0.0000i	0.5000 + 0.0000i

Table 6. Novel Fourier transform of shape, Fig. 1(a).

U	V	W
-0.4921 - 0.7487i	-0.5303 - 0.6307i	-0.0221 - 0.4903i
-0.2222 + 0.3724i	-0.0256 + 0.3908i	-0.4622 + 0.0392i
-0.0484 + 0.1828i	-0.1290 - 0.0750i	0.0469 + 0.4181i
0.4710 + 0.0883i	0.2302 + 0.3172i	0.3617 - 0.0419i
-0.2039 - 0.4313i	0.1550 - 0.3088i	-0.0219 - 0.2978i
-0.0324 + 0.1929i	-0.0992 - 0.2095i	-0.2318 - 0.0135i

Table 7. Novel Fourier transform of shape, Fig. 1(b).

U	V	W
-0.4921 - 0.7487i	-0.5303 - 0.6307i	-0.0221 - 0.4903i
-0.2222 + 0.3724i	-0.0256 + 0.3908i	-0.4622 + 0.0392i
-0.0484 + 0.1828i	-0.1290 - 0.0750i	0.0469 + 0.4181i
0.4710 + 0.0883i	0.2302 + 0.3172i	0.3617 - 0.0419i
-0.2039 - 0.4313i	0.1550 - 0.3088i	-0.0219 - 0.2978i
-0.0324 + 0.1929i	-0.0992 - 0.2095i	-0.2318 - 0.0135i

6.2. Rotation effect

In this case, we show invariant of the new Fourier transform under rotation. For this we apply rotation for shape, Fig. 1(a), under direction x-axis, so we use in this experiment Eq. (24) with $\theta = \frac{\pi}{3}$ radians = 60 degrees. The rotate can also be applied with y-axis and z-axis using Eqs. (25) and (26). The coordinates of shape rotated are defined in Eq. (27). Table 8 shows results with our method of coordinates x for 3D point sets and it's rotated (for shape Fig. 1(a), and its rotated shape); we note that novel Fourier is invariant with rotation.

$$R_x(\theta) = \begin{pmatrix} 1 & 0 & 0 \\ 0 & cos\theta & -sin\theta \\ 0 & sin\theta & cos\theta \end{pmatrix} \tag{24}$$

$$R_y(\theta) = \begin{pmatrix} cos\theta & 0 & sin\theta \\ 0 & 1 & 0 \\ -sin\theta & 0 & cos\theta \end{pmatrix} \tag{25}$$

$$R_z(\theta) = \begin{pmatrix} cos\theta & -sin\theta & 0 \\ sin\theta & cos\theta & 0 \\ 0 & 0 & 1 \end{pmatrix} \tag{26}$$

So, by applying R_x transform

$$\begin{cases} x_r = x \\ y_r = ycos\theta - zsin\theta \\ z_r = ycos\theta + zsin\theta \end{cases} \tag{27}$$

Table 8. Novel Fourier transform of coordinates x.

U (shape Fig. 1(a)	U (rotated shape)
-0.4921 - 0.7487i	-0.4921 - 0.7487i
-0.2222 + 0.3724i	-0.2222 + 0.3724i
-0.0484 + 0.1828i	-0.0484 + 0.1828i
0.4710 + 0.0883i	0.4710 + 0.0883i
-0.2039 - 0.4313i	-0.2039 - 0.4313i
-0.0324 + 0.1929i	-0.0324 + 0.1929i

6.3. Affinity effect

In this case, we show invariance of the new Fourier transform under affinity. For this experiment we have used affinity 3D matrix Eq. (28). We consider coordinates of transformed shape in Eq. (29). The nine coefficients a_{ij} are not at all independent of one another, because their relationship will depend on the conditions of invariance that we establish. Table 9 shows results with our method of coordinates y for 3D point sets and its transformed (for shape, Fig. 1(a) and its transformed shape); we note that novel Fourier give a good results.

$$A = \begin{pmatrix} a_{11} & a_{12} & a_{13} \\ a_{21} & a_{22} & a_{23} \\ a_{31} & a_{32} & a_{33} \end{pmatrix} \tag{28}$$

So

$$\begin{cases} x_a = a_{11}x + a_{12}y + a_{13}z \\ y_a = a_{21}x + a_{22}y + a_{23}z \\ z_a = a_{31}x + a_{32}y + a_{33}z \end{cases} \tag{29}$$

Table 9. Novel Fourier transform of coordinates *y*.

V (shape Fig. 1(a)	*V* (transformed shape)
-0.5303 - 0.6307i	-0.5303 - 0.6307i
-0.0256 + 0.3908i	-0.0256 + 0.3908i
-0.1290 - 0.0750i	-0.1290 - 0.0750i
0.2302 + 0.3172i	0.2302 + 0.3172i
0.1550 - 0.3088i	0.1550 - 0.3088i
-0.0992 - 0.2095i	-0.0992 - 0.2095i

6.4. Application on 3D curve

In this subsection, we apply our new Fourier of 3D curve. As shown in Fig. 2(a) synthetic contour represent 3D curve was created using the parametric Eq. (30) and in Fig. 2(b) the noised curve (Gaussian noise distribution is added here):

$$\begin{cases} x(t) = 2\cos(t) \\ y(t) = 0.5\sin(5t) \qquad with\ t \in [0, 2\pi] \\ z(t) = 3\sin(t) \end{cases} \tag{30}$$

with *x (t)*, *y (t)* and *z (t)*: are Cartesian coordinates of parametric curve of period 2π.

(a) **Original 3D parametric curve.**   (b) **Noisy 3D parametric curve.**

Fig. 2. Original and noisy 3D parametric curve.

This experiments will demonstrate the effect of noise in this case (Fig. 2). Table 10 shows results with our new Fourier transform; we note that novel Fourier is robust under noise effect.

6.5. Rotation effect

In this experiment we show rotation effect of our new Fourier transform in the case of 3D curve. Table 11 shows results with our new Fourier transform for coordinates *x* for 3D curve (Fig. 2) and its rotated shape; we note that novel Fourier is invariant under rotation effect (|x| denote module of *x*).

Table 10. Results $abs\big|\log(U)\big|$ **for Fig. 2(a) and** $abs\big|\log(U)\big|$
for Fig. 2(b) of coordinates *x* **of original and noisy 3D curve.**

$abs\big|\log(U)\big|$, Fig. 2(a)	$abs\big|\log(U)\big|$, Fig. 2(b)
1.4374	1.4349
2.6127	2.6097
2.5980	2.5985
1.4240	1.4213
0.6923	0.6746
1.4507	1.4342
2.6274	2.6123
2.5833	2.5809
1.4106	1.3952
0.6925	0.6302

Table 11. Novel Fourier transform of coordinates *x*.

U (3D curve Fig. 2(a))	*U* (rotated 3D curve)
-1.0026 - 1.7299i	-1.0026 - 1.7299i
-0.9940 + 1.7349i	-0.9940 + 1.7349i
1.9994 - 0.0099i	1.9994 - 0.0099i
-1.0111 - 1.7249i	-1.0111 - 1.7249i
-0.9853 + 1.7397i	-0.9853 + 1.7397i
1.9992 - 0.0199i	1.9992 - 0.0199i

6.6. Affinity effect

The same for 3D point set we show effect of affinity of our new Fourier in the case of 3D curve. Table 12 shows results with our new Fourier of coordinate *z* for 3D curve (Fig. 2) and its transformed shape (for 3D curve, Fig. 2(a) and its transformed shape); we note that novel Fourier is invariant under general affine transform which is not the case using classic transforms.

Table 12. Novel Fourier transform of coordinates *z*.

W (3D curve Fig. 2(a))	*W* (transformed 3D curve)
-0.0296 - 0.0509i	-0.0296 - 0.0509i
-0.0292 + 0.0512i	-0.0292 + 0.0512i
0.0589 - 0.0005i	0.0589 - 0.0005i
-0.0300 - 0.0507i	-0.0300 - 0.0507i
-0.0288 + 0.0514i	-0.0288 + 0.0514i
0.0589 - 0.0010i	0.0589 - 0.0010i

7. Conclusions

Many works have used the non-uniform Fourier transform [20, 21]. The problem treated in this new work is not the spacing between samples, but simply the order change of points in storage or manipulation of those points. This paper presents a new Fourier transform to solve the issue related to point's indexes. The radius parameter is used in the development process. The obtained experimental results on a set of 3D points and 3D curve are satisfactory. Shift theorem is available

only where the Shift is linear, but when the order of points is random this theorem becomes invalid. In future work, we are planning to implement new moments and to apply our approach to 3D objects (Mesh).

References

1. Bustos, B.; Keim, D.A.; Saupe, D.; Schreck, T.; and Vranić, D.V. (2005). Feature-based similarity search in 3D object databases. *ACM Computing Surveys (CSUR)*, 37(4), 345-387.

2. Funkhouser, T.; Min, P.; Kazhdan, M.; Chen, J.; Halderman, A.; Dobkin, D.; and Jacobs, D. (2003). A search engine for 3D models. *ACM Transactions on Graphics (TOG)*, 22(1), 83-105.

3. Fisher, M.; and Hanrahan, P. (2010). Context-based search for 3D models. *In ACM Transactions on Graphics (TOG) ACM*, 29(6), p. 182.

4. Qian, Y.; Hui, R.; and Gao, X. (2013). 3D CBIR with sparse coding for image-guided neurosurgery. *Signal Processing*, 93(6), 1673-1683.

5. Arakeri, M.P.; and Reddy, G.R.M. (2012). A novel CBIR approach to differential diagnosis of liver tumor on computed tomography images. *Procedia Engineering*, 38, 528-536.

6. Di Mascio, T.; Frigioni, D.; and Tarantino, L. (2010). VISTO: A new CBIR system for vector images. *Information Systems*, 35(7), 709-734.

7. Shih, J.L.; Liu, Y.H.; and Tsao, F.C. (2013). Combination of 3D discrete Fourier transform and 3D angular radial transform for 3D model retrieval. *Journal of Information Technology and Applications*, 7(1), 21-29.

8. Lmaati, E.A.; El Oirrak, A.; Kaddioui, M.N.; Ouahman, A.A; and Sadgal, M. (2010). 3D model retrieval based on 3D discrete cosine transform. *The International Arab Journal of Information Technology*, 7(3), 264-270.

9. Dutagaci, H.; Godil, A.; Sankur, B; and Yemez, Y. (2010). View subspaces for indexing and retrieval of 3d models. In IS&T/SPIE Electronic Imaging. *International Society for Optics and Photonics*, 75260M-75260M.

10. Tangelder, J.W.; and Veltkamp, R.C. (2008). A survey of content based 3D shape retrieval methods. *Multimedia tools and applications*, 39(3), 441-471.

11. El Oirrak A., Aboutajdine D. ; and Daoudi M. (2002). Estimation of general affine motion using Fourier descriptors, *Pattern Recognition*, 35(1), 223-228.

12. El Oirrak A., Aboutajdine D.; and Daoudi M. (2003). Affine invariant descriptors for color images using Fourier series, *Pattern Recognition Letters*, 24, 1339-1348.

13. Scheib, V.; Haber, J.; Lin, M.C.; and Seidel, H.P. (2002). Efficient fitting and rendering of large scattered data sets using subdivision surfaces. *In Computer Graphics Forum Blackwell Publishing*, Inc., 21(3), 353-362.

14. Amidror, I. (2002). Scattered data interpolation methods for electronic imaging systems: a survey. *Journal of electronic imaging*, 11(2), 157-176.

15. Hu, M.K. (1962). Visual pattern recognition by moment invariants, *IRE Transactions on Information Theory,* 179-187.

16. Fessler, J.; and Sutton, B.P. (2003). Nonuniform fast Fourier transforms using min-max interpolation. *IEEE Transactions* on *Signal Processing*, 51(2), 560-574.

17. Sabhara, R.K.; Lee, C.P.; and Lim, K.M. (2013). Comparative study of hu moments and zernike moments in object recognition. *SmartCR*, 3(3), 166-173.

18. Vizitiu, C.I.; Munteanu, D.; and Molder, C. (2008). A new version of Flusser moment set for pattern feature extraction. *WSEAS Transactions on Information Science and Applications*, 5(4), 396-406.

19. Mokhtarian, F.; and Abbasi, S. (2001). Affine curvature scale space with affine length parametrisation. *Pattern Analysis and Applications*, 4(1), 1-8.

20. Bagchi, S.; and Mitra, S.K. (2012). The nonuniform discrete Fourier transform and its applications in signal processing. *Springer Science & Business Media*, 463.

21. Flusser J.; and Suk T. (1993). Pattern recognition by affine moment invariants. *Pattern recognition*, 26(1), 167-174.